Arabian Journal of Geosciences (2021) 14: 2182
https://doi.org/10.1007/s12517-021-08544-8

ORIGINAL PAPER

# An integrated study on stability assessment of the Seyrantepe underground openings (Gaziantep, Turkey)

**Serdar Allı[1] · Hanifi Çanakçı[2] · Melih Geniş[3]**

Received: 29 March 2021 / Accepted: 28 September 2021 / Published online: 20 October 2021


**Abstract**
In view of the geotechnical engineering and engineering geology, the Seyrantepe underground openings have important characteristics. Although these underground openings have thin roof thickness, large parallel span, thin pillars and low rock mass strength, they are standing up for years. Due to the rock masses being complicated and inhomogeneous material and containing discontinuities, it is commonly difficult to obtain the required mechanical parameters for the analyses. In this paper, a combined analysis, including failure-based back analysis, Hoek–Brown and Mohr–Coulomb failure criteria, was executed to determine the cohesion, frictional angle and tensile strength of the rock mass. Integrated numerical, analytical and empirical analyses were performed to assess the stability of the underground openings, which were excavated from limestone. The effects of the adjacent openings on the stability and failure zones were also investigated. The analysis shows that considerably important parameter for the roof stability is the tensile strength of the rock mass. While the lowest tensile strength is obtained from Hoek–Brown criterion, Mohr–Coulomb criterion gives the highest tensile strength. Numerical analysis shows that adjacent openings affect the stability and failure process. According to the bending theory, the limit of the roof span ranges between 11 and 22.5 m depending on roof thicknesses of 9 and 25 m, respectively. Although these underground openings are standing for a long time, results of the analyses show that some protective measures against instability are necessary.

**Keywords** Underground openings · Stability analysis · Analytical analysis · Back analysis · FEM · Limestone

## Introduction

Gaziantep is one of the most important historical cultural cities of southeastern Turkey. The geological formation of the city is mainly limestone. The ability to easily cut, shape and use limestone as a building material has enabled the creation of many artificial underground openings. Stone used for the construction of houses in the city was supplied by creating underground openings that provided the opportunity to work in both the summer and winter. Most of the time, basements were made by excavating rock when houses were built, and the stones obtained were later used for houses. Today, most of these underground openings are old abandoned quarries excavated for supplying stone to Gaziantep and the surrounding vicinity. The Seyrantepe underground openings are one of the largest abandoned quarries of the city.

The Seyrantepe underground openings are located in Şehitkamil district of Gaziantep. The openings were excavated in a small hill and are three levels (Fig. 1). Currently, the Gaziantep Metropolitan Municipality is considering using these openings as a historical museum; however, instability is a major concern.

The underground openings have the following characteristics: thin roof thickness, large parallel span, thin pillars, low rock mass strength and being unsupported for years. Although the openings excavated from limestone have survived and maintained their original integrity for years, there is some indication of yielding and partial collapse on

Communicated by Zeynal Abiddin Erguler.

✉ Serdar Allı
salli@bartin.edu.tr

[1] Department of Civil Engineering, Bartın University, Bartın 74100, Turkey

[2] Department of Civil Engineering, Hasan Kalyoncu University, Gaziantep 27010, Turkey

[3] Department of Mining Engineering, Zonguldak Bülent Ecevit University, Zonguldak 67100, Turkey

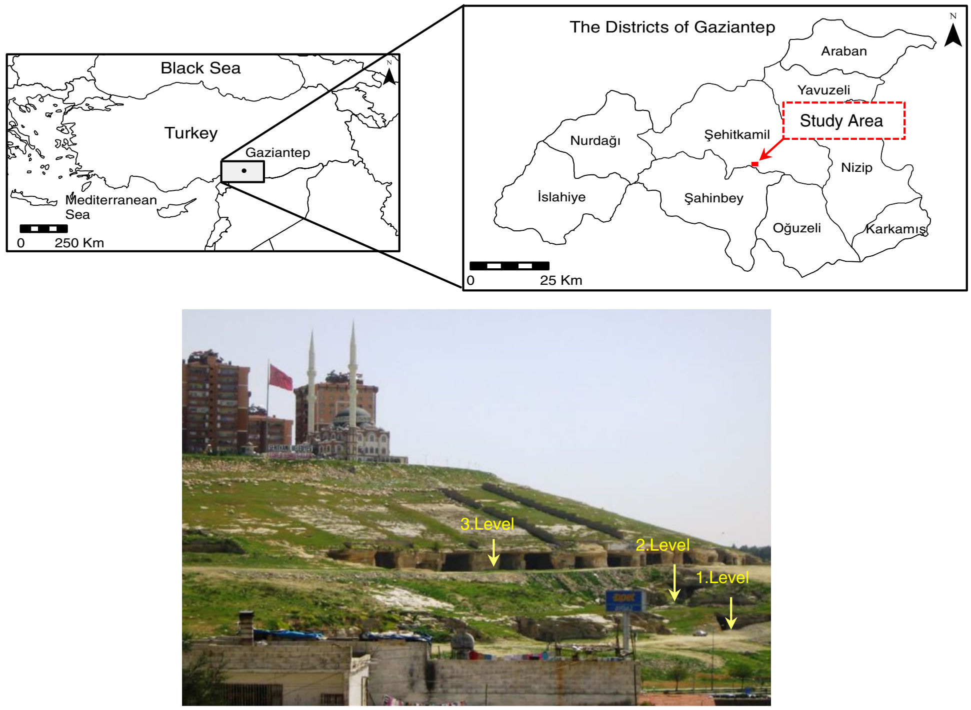


**Fig. 1** Location and general view of the Seyrantepe underground openings

different scales at several locations. Stability is the main geotechnical problem with these underground openings.

Many studies were conducted to investigate instability problems in underground openings. Waltam and Park (2002) investigated the stability of three lava tubes in Cheju Island, South Korea. They suggested a ratio of tube width to roof thickness for checking the stability of the lava tubes. Canakci (2007) investigated the possible causes of two collapsed caves in Gaziantep, Turkey. Similar to Waltam and Park (2002), Hatzor et al. (2010) discussed the stability of shallow karstic caves in blocky rock masses. Suchowerska et al. (2012) investigated the roof collapse of underground cavities for different rock properties and geometries using Hoek–Brown failure criterion. They presented stability charts to predict the roof collapse of underground cavities. Ulusay et al. (2013) investigated the short- and long-term stability of Avanos Underground Congress Centre carved into soft Tuffs in Cappadocia, Turkey. They performed experimental, numerical and analytical analyses. Additionally, an in situ monitoring program was conducted to investigate crack propagation.

This paper assesses the stability of the Seyrantepe underground openings and discusses the stability problems encountered in the underground openings. First, laboratory tests were performed on rock core samples to determine the physical and mechanical properties of the intact rock. Then, the geotechnical properties of the rock mass were evaluated through rock mass classification systems. The Geomechanics Classification (RMR), the Geological Strength Index (GSI) and Rock Quality Index (Q) were used for rock mass classification. A combined analysis, including back analysis, Hoek–Brown and Mohr–Coulomb failure criteria, was conducted to determine the geotechnical parameters of the rock mass. Finally, the stability of the manmade underground openings was evaluated using numerical, analytical and empirical methods, and the results are discussed along with the field observations.

## Geology

The general geology of Gaziantep was defined by Tolun and Pamir (1975), Terlemez et al. (1997), MTA (1997) and Coşkun and Coşkun (2000). The geological formations of the provincial settlement mainly involve Yavuzeli (Ty), Firat (m1) and Gaziantep (e) formations. A Yavuzeli formation consists of reddish dark brown, dark grey and blackish, unbedded, partly quite thick, porous basalt deposits that have thickness of approximately 50 m. A Firat formation, unconformably underlying the Yavuzeli formation, has a whitish, dingy yellow coloured, thin- to thick-bedded, partly unbedded reefal limestone. A Gaziantep formation, conformably underlying the Firat formation, consists of clayey limestone, limestone and chalky limestone. It shows changing features and has a thickness of approximately 100–250 m. It is from the Latest Eosen (Priabonian) and Early Oligocene (Stampian) Epochs, as determined by Terlemez et al. (1992). Most of the underground openings in the city occur in Gaziantep and Firat formations.

According to a visual geological investigation, the Seyrantepe underground openings are located in the Gaziantep formation, which includes whitish to light grey and/or beige, soft strong, fresh to slightly weathered, thin- to thick-bedded, almost horizontal clayey, locally massive, marly limestone (Fig. 2). The rock mass is extremely massive. The joints are not closely spaced, according to ISRM (2007), and the persistence of the joints is rare. The bedding is widely spaced and nearly horizontal (Fig. 3a, b).

## Stability problems observed in the underground openings

The Seyrantepe underground quarry has adjacent parallel openings. The upper level includes eight large openings and seven small openings. Figure 4 shows the plan and inner view of the underground openings on the third level. The spans of the underground quarry change between 5 and 55 m, and average heights are 5.6 m. The openings are connected to each other from the inside on the levels. The cross section is approximately rectangular. The roofs are declined following bedding planes so that roof thickness varies from 2 to 30 m. Each opening has pillars to support its roof rock.

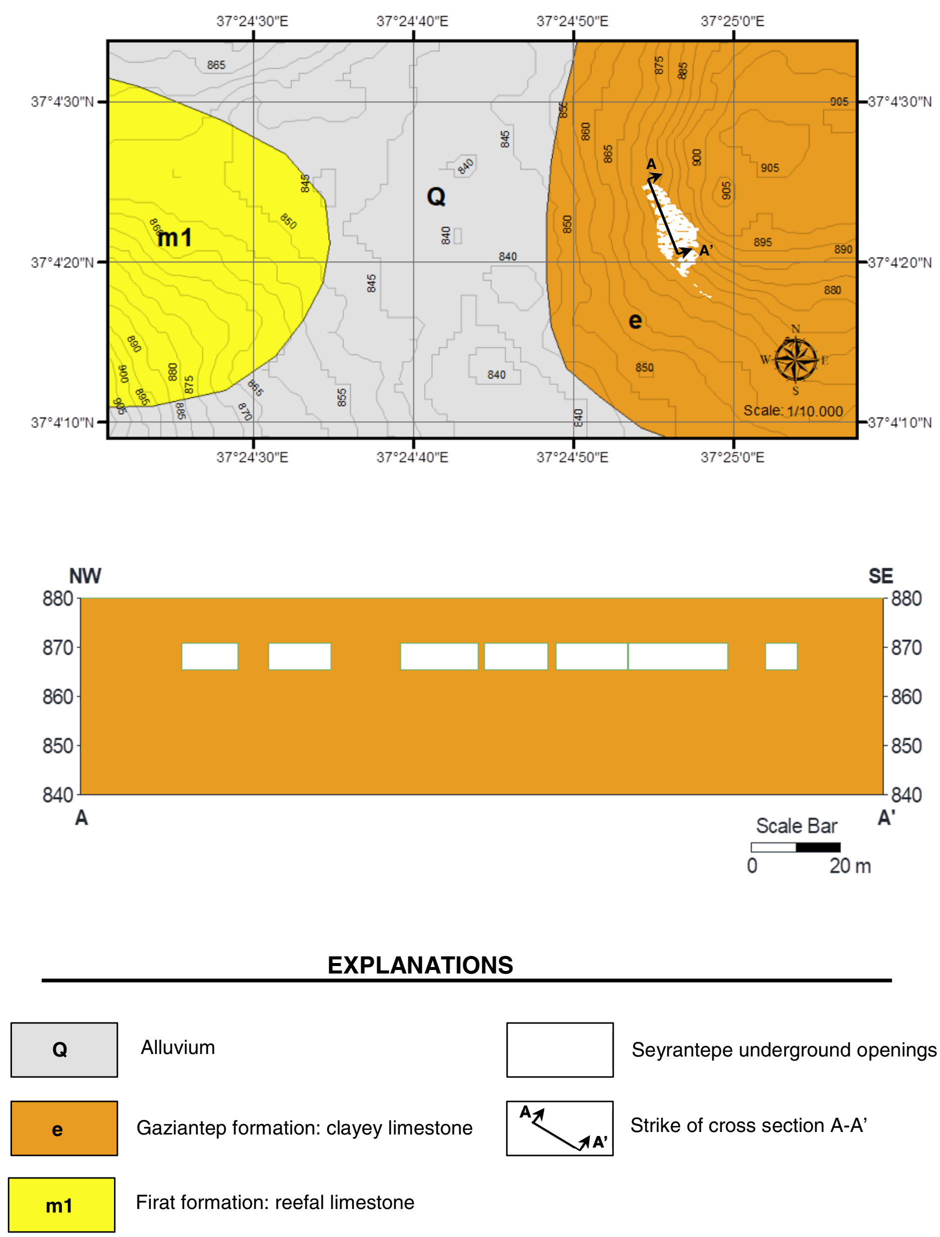


Fig. 2 Geological map and cross sections of the upper level of Seyrantepe underground openings (modified from MTA 1997)


**Fig. 3** Horizontal bedding of the Seyrantepe underground openings

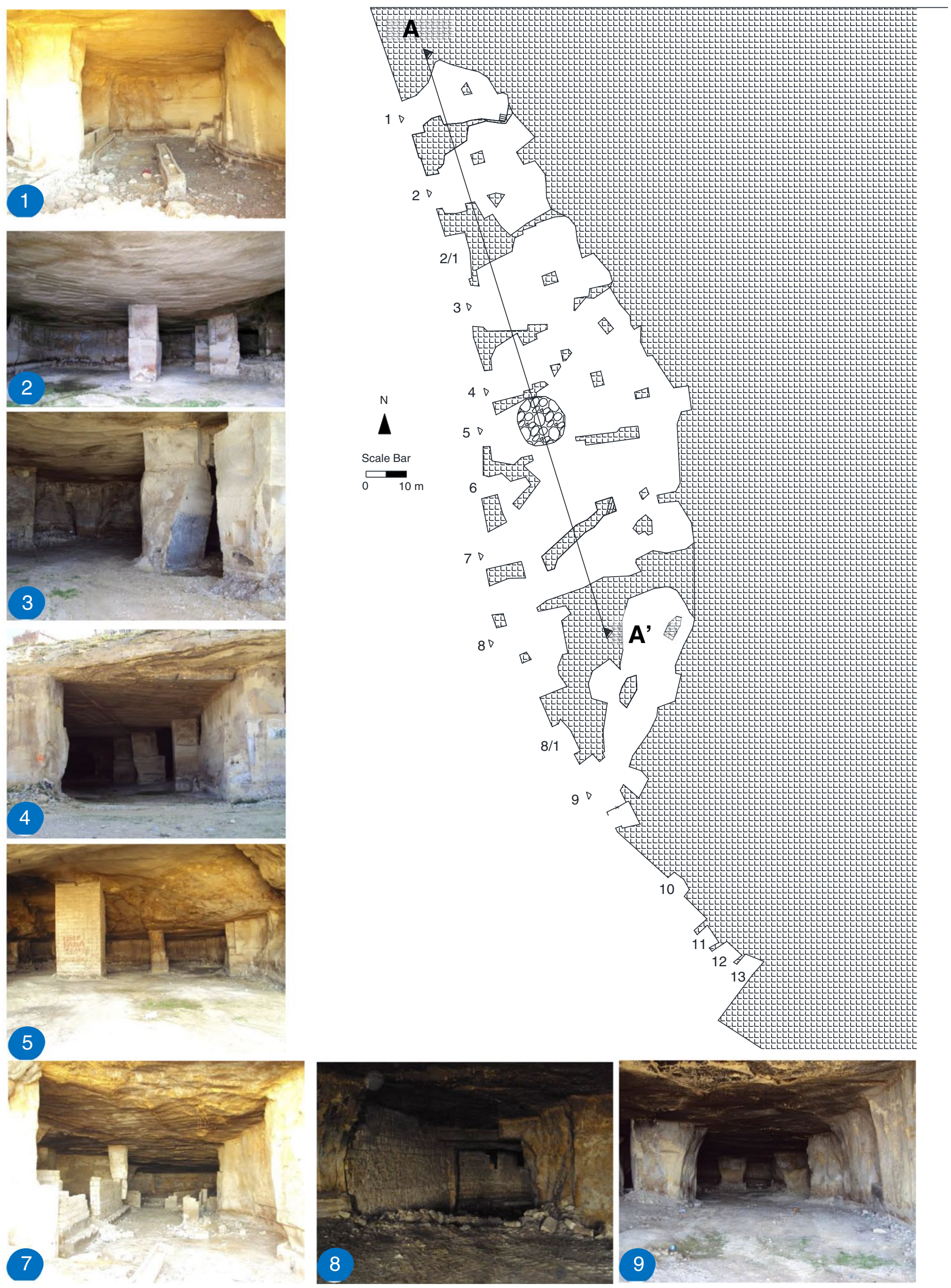


**Fig. 4** The plan and inner views of the third level of the Seyrantepe underground openings

Although the underground openings have stood for years, some stability problems were observed.

According to the authors' observations, stability is affected by the following factors.

1. Stress-induced failures are the stability problems that are most commonly observed in these underground openings. This type of failure occurs when the induced stress is greater than the strength of the rock mass. The failure can be shear or tension. There are some shear failures that developed in the rock pillars between the openings. Figure 5a shows the shear failure observed at the rock pillar between openings 3 and 4. Typical stress-induced failures occur in wide roof spans against thin roof thicknesses due to over-bending stress. An example is the collapsed roof of the entrance of opening 8, as seen in Fig. 5b.

   A roof collapse was also observed at the entrance of opening 5. A general view of opening 5 before and after the collapse of the roof is presented in Fig. 6a and b. Debris materials are clearly seen in Fig. 6b. The spalling of the roof can also be seen; the spalling of rock is an indication of stress-dependent behaviour.

2. Weathering is another important factor affecting the openings' stability. There is no sufficient drainage system around the underground openings for the discharge of surface water and the rock mass is exposed to atmospheric effects. With time, weathering tends to reduce

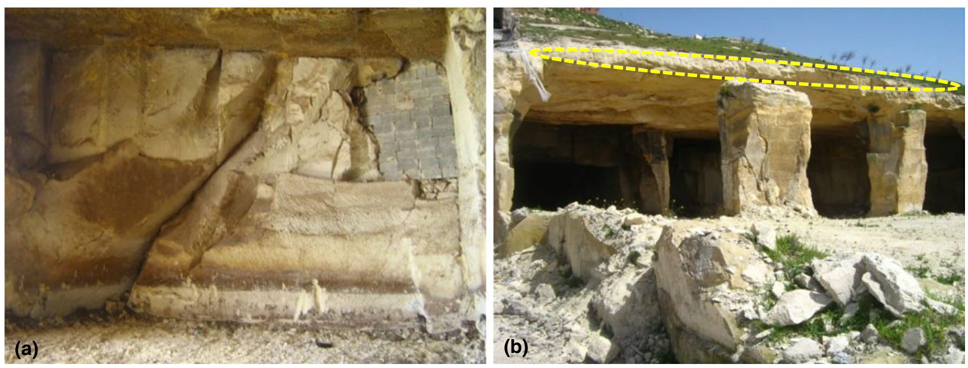


**Fig. 5** Some examples of stress-induced failures. **a** Shearing at the rock pillars between openings 3 and 4, **b** the collapsed roof of the entrance of opening 8


**Fig. 6** General views of opening 5. **a** Before the collapse, **b** after the collapse

strength and turns the colour of the rock mass. Signs of this weakening are clearly observed at different locations in the openings (Fig. 7a, b, c, d).

3. The cracks that have developed in some locations possibly affect the openings' stability. Time-dependent strength reduction of the rock mass, additional external loads such as new buildings around the openings, earthquake loads and so on, or over stresses in the rock mass, can induce crack formations. Specifically, crack propagation in a rock mass is a precursory sign of failure. In the Seyrantepe underground openings, cracks mainly develop in the roofs and pillars (Fig. 8a, b, c).

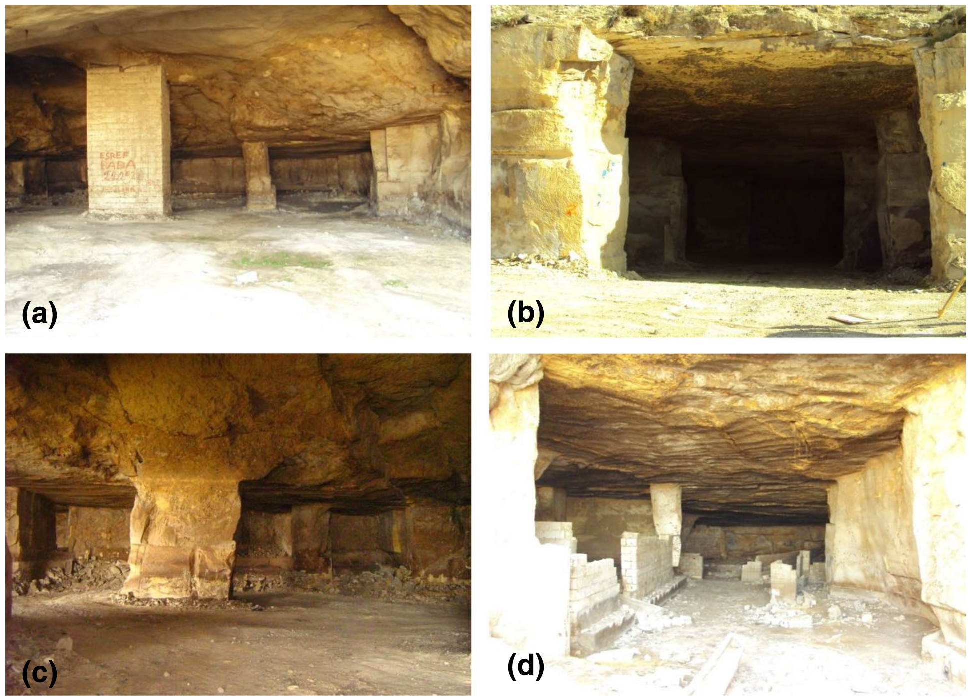


**Fig. 7** Weathering of the rock surfaces. **a** The roof of opening 5, **b** the entrance of opening 3, **c** the roof of opening 4, **d** the roof of opening 7

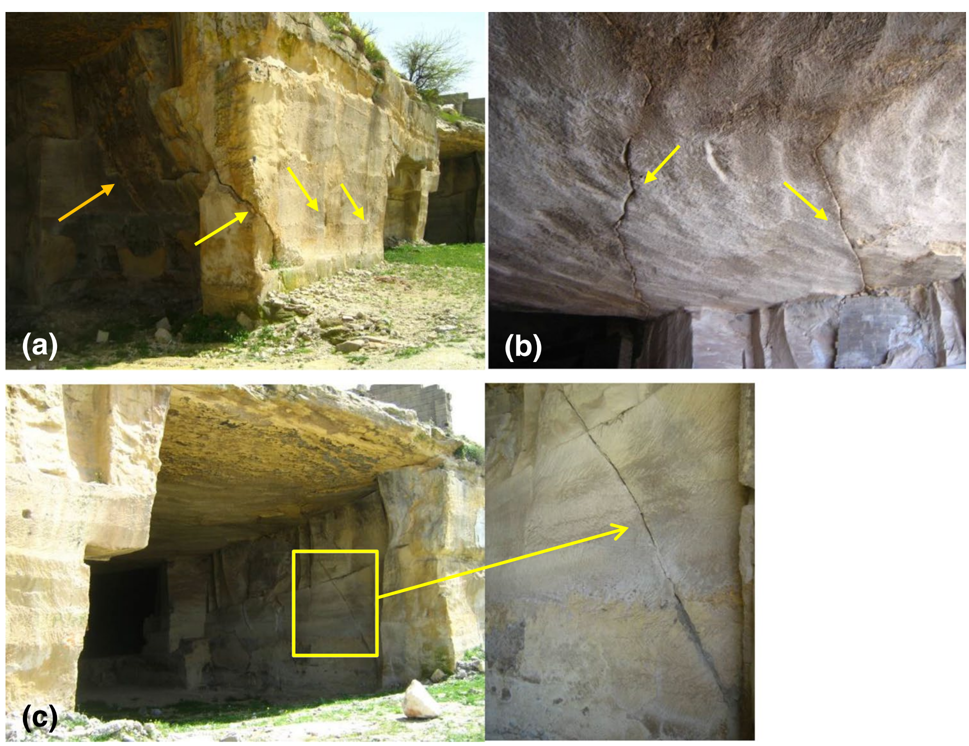


**Fig. 8** Some examples of the cracks developed in the pillars and roof. **a** The outside pillar of opening 2, **b** the roof of opening 3, **c** the pillars between openings 3 and 4

## Rock mass classification

Using rock mass classification systems, unsupported standing time, support requirements and support pressure can be empirically determined for underground spaces excavated in rock masses. There are numerous classification systems used today. The most commonly used systems are suggested in the studies of Lauffer (1958), Deere and Miller (1967), Wickham et al. (1972), Bieniawski (1989), Barton et al. (1974), Grimstad and Barton (1993), Hoek et al. (1995), Sonmez and Ulusay (2007) and Aydan et al. (2014).

In this study, rock mass classification systems such as the RMR (Bieniawski 1989), Q (Barton et al. 1974; Grimstad and Barton 1993) and GSI (Hoek et al. 1995; Sonmez and Ulusay 2007) were employed to characterize the rock mass and to estimate the rock mass strength parameters of the Seyrantepe underground openings. The values of classification systems were computed in terms of the worst and best conditions of the area, and the results are presented in Table 1. A range of the rock mass values was considered in place of a single value to overcome some of the uncertainties of the classification systems.

## Determination of the geotechnical parameters

The main problem encountered in designing and analysing underground structures is to determine in situ strength and deformation parameters. Specifically, due to discontinuities in rock mass, there are some experimental difficulties in determining these parameters. Sampling of the rock mass, along with discontinuities for laboratory experiments, creates significant difficulties in determining the strength and deformation parameters of the rock masses. To overcome this, some laboratory tests, such as the uniaxial compression test, can be performed on intact rock samples, and in situ geotechnical parameters can be computed by including rock mass classification systems in the calculations.

In this study, basic laboratory tests were conducted to determine the intact rock properties of the Seyrantepe underground openings. Due to the lack of cohesion, frictional angle and tensile strength of the rock mass, a combined analysis, including back analysis, Hoek–Brown and Mohr Coulomb failure criteria, was conducted. The details are presented in the following subsections.

**Table 1** Rock mass classification for limestone

| Classification | Rating range | Average value |
|---|---|---|
| Geomechanics Classification (RMR) | 77–83 | 80 |
| Rock Quality Index (Q) | 39.1–76.2 | 57.6 |
| Geological Strength Index (GSI) | 85 | 85 |

## Laboratory tests

To determine the necessary geotechnical parameters for rock mass, drillings were performed in the field, and rock mechanics tests were conducted on 20 good-quality rock core samples obtained from the borings. The tests involved the determination of unit weight (γ), uniaxial compressive strength (UCS), modulus of elasticity (E), Poisson's ratio ($\nu$) and water content (w) of the surrounding limestone as intact rock under both dry and fully saturated conditions. These tests were conducted in accordance with the test procedures suggested by the ISRM (2007). The results of the tests are presented in Table 2. Under dry conditions, the average values of unit weight, uniaxial compressive, modulus of elasticity and Poisson's ratio are 18.3 kN/m$^3$, 4.08 MPa, 9.85 GPa and 0.18, respectively. Under fully saturated conditions, the average values of unit weight, water content (%), uniaxial compressive, modulus of elasticity and Poisson's ratio are 21.5 kN/m$^3$, 18.4%, 2.64 MPa, 8.11 GPa and 0.13, respectively. It is clear from Table 2 that, under fully saturated conditions, a decrease of more than 60% occurs in strength compared with dry conditions. In terms of strength and deformability, the intact rock is extremely weak, according to the ISRM (2007).

It should be noted that the strength values given in Table 2 were obtained from intact core samples, but the rock mass strength of the limestone is expected to be lower than that of the intact rock due to the rock mass quality. To calculate the shear strength parameters and tension strength of the rock mass, this case was considered by means of rock mass classification systems. Then, the calculated values were compared with failure-based back analysis results.

## Determination of the rock mass geotechnical parameters considering Hoek–Brown failure criterion

Using the relationship between the Hoek–Brown and Mohr–Coulomb criteria, the strength and deformation parameter of the Seyrantepe underground openings were obtained. The Hoek–Brown input parameters are Geological Strength Index (GSI), the rock mass disturbance factor ($D$), Hoek–Brown material constant of intact rock ($m_i$), uniaxial compressive strength of intact rock $\left(\sigma_{ci}\right)$ and modulus of elasticity of intact rock ($E_{\text{i}}$).

**Table 2** Laboratory test results performed on the core samples obtaining from the borings

| Borehole no | Sample depth (m) | Unit weight (kN/m$^3$) | Water content (%) | UCS (MPa) | Modulus of elasticity, Ei (GPa) | Poisson's ratio |
|---|---|---|---|---|---|---|
| Sk-1 saturated | 2 | 21.7 | 18.7 | 2.74 | 8.0 | 0.12 |
| Sk-2 saturated | 3 | 21.7 | 18.0 | 2.79 | 8.2 | 0.13 |
| Sk-3 saturated | 2 | 21.3 | 18.2 | 2.67 | 8.4 | 0.14 |
| Sk-4 saturated | 3 | 21.5 | 18.6 | 2.60 | 8.1 | 0.13 |
| Sk-5 saturated | 2 | 21.6 | 19.1 | 2.61 | 7.9 | 0.14 |
| Sk-6 saturated | 3 | 21.6 | 19.6 | 2.54 | 8.3 | 0.12 |
| Sk-7 saturated | 2 | 21.7 | 17.2 | 2.60 | 8.4 | 0.12 |
| Sk-8 saturated | 3 | 21.4 | 17.3 | 2.56 | 8.0 | 0.13 |
| Sk-9 saturated | 2 | 21.3 | 18.4 | 2.60 | 7.9 | 0.14 |
| Sk-10 saturated | 3 | 21.5 | 18.4 | 2.70 | 7.9 | 0.11 |
| *Average saturated* | | *21.5* | *18.4* | *2.64* | *8.11* | *0.13* |
| Sk-1 dry | 2 | 18.4 | - | 4.07 | 9.2 | 0.17 |
| Sk-2 dry | 3 | 18.3 | - | 4.17 | 10.3 | 0.19 |
| Sk-3 dry | 2 | 18.5 | - | 4.02 | 9.1 | 0.18 |
| Sk-4 dry | 3 | 18.1 | - | 3.92 | 9.8 | 0.17 |
| Sk-5 dry | 2 | 18.4 | - | 4.21 | 9.9 | 0.18 |
| Sk-6 dry | 3 | 18.3 | - | 4.24 | 10.1 | 0.19 |
| Sk-7 dry | 2 | 18.4 | - | 4.00 | 10.2 | 0.20 |
| Sk-8 dry | 3 | 18.5 | - | 4.03 | 10.5 | 0.19 |
| Sk-9 dry | 2 | 18.1 | - | 4.11 | 9.5 | 0.18 |
| Sk-10 dry | 3 | 18.2 | - | 4.00 | 9.9 | 0.19 |
| *Average dry* | | *18.3* | | *4.08* | *9.85* | *0.18* |

The Geological Strength Index (GSI) developed by Hoek (1994) introduces a number which can be used for the estimation of rock mass strength from the lithology, structure and surface conditions of the discontinuities. During the early years of the GSI, it was estimated directly from RMR. The correlation between RMR and GSI has proved to be unreliable over the years. Therefore, it is recommended that GSI should be evaluated directly from the charts presented by Hoek and Marinos (2000). The rock mass surrounding the Seyrantepe underground openings is extremely massive marly limestone, which includes few widely spaced discontinuities with very rough to rough, fresh to slightly weathered surface. So an average GSI value of 85 is considered from the chart introduced by Hoek and Marinos (2000)

*D* is a parameter which is related to the degree of disturbance due to stress relaxation and blast damage. The value of *D* is ranged from 0 for undisturbed rock masses to 1 for very disturbed rock masses. Hoek and Brown (2019) present some cases in which the control of blasting and method of excavation are of considerable importance. Hoek and Brown (2019) suggest $D = 0$ for excellent quality-controlled blasting or excavation by a road-header or tunnel boring machine and mechanical or hand excavation in poor-quality rock masses due to resulting in minimal disturbance to the surrounding rock mass. Since the Seyrantepe underground openings were excavated in soft marly limestone by hand and machinery using traditional tools and no blasting, the rock mass disturbance factor (D) is assumed to be 0.

Hoek–Brown material constant ($m_i$), uniaxial compressive strength $\left(\sigma_{ci}\right)$ and modulus of elasticity ($E_{\mathrm{i}}$) are the constants related to the intact rock which are used in Hoek–Brown failure criterion. Wherever possible, the values of these constants are obtained by statistical analysis of the results of a set of triaxial tests on core samples. When the triaxial tests are not available the values of $m_i$, $\left(\sigma_{ci}\right)$ and $E_i$ can be estimated from the tables suggested by Hoek (2007).

Hoek (2007) suggests $m_i = 9 \pm 2$ for micritic limestones, $10 \pm 2$ for sparitic limestones, $12 \pm 3$ for crystalline limestone and $7 \pm 2$ for marls. Since the rock mass surrounding the Seyrantepe underground openings is marly limestone, Hoek–Brown constant ($m_i$) is estimated to be 10 from the table suggested by Hoek (2007) due to no triaxial test results. The average uniaxial compressive strength of the intact rock $\left(\sigma_{ci}\right)$ and the average modulus of elasticity of intact rock ($E_{\mathrm{i}}$) are calculated from the results of uniaxial compressive strength tests on dry core samples as 4.08 MPa and 9.85 GPa, respectively.

The RocLab (v.1.0) software (Rocscience 2002) was used to determine the internal friction angle, cohesion, tensile strength and modulus of elasticity of the rock mass. These parameters were then compared with the parameters obtained from the back analysis. Table 3 presents the geotechnical properties

**Table 3** Geotechnical properties of the Seyrantepe underground openings as determined by RocLab software

| Geotechnical properties | Value |
|---|---|
| Intact rock strength ($\sigma_{ci}$; MPa) | 4.08 |
| Uniaxial compression strength of the rock mass ($\sigma_{cm}$; MPa) | 1.77 |
| Hoek–Brown constant $m_\mathrm{i}$ | 10 |
| Average GSI value | 85 |
| Disturbance factor, $D$ | 0 |
| Elastic modulus of the intact mass ($E_i$; GPa) | 9.85 |
| Hoek–Brown constant $m_b$ | 5.853 |
| Hoek–Brown constant $s$ | 0.1889 |
| Hoek–Brown constant $a$ | 0.5 |
| Elastic modulus of the rock mass ($E_m$; GPa) | 9.13 |
| Cohesion ($c_m$; kPa) | 322 |
| Internal friction angle ($\phi_m$;°) | 47.3 |
| Rock mass tensile strength (kPa) | 132 |

of the rock mass according to the generalized Hoek–Brown failure criterion. The cohesion, internal friction angle, tensile strength and elastic modulus of the rock mass with GSI = 85, $m_i = 10$, $D=0$, $\sigma_{ci}= 4.08$ MPa and $E_\mathrm{i}= 9.85$ GPa are calculated as 322 kPa, 47.3°, 132 kPa and 9.13 GPa, respectively.

## Determination of the rock mass geotechnical parameters considering Mohr–Coulomb failure criterion

Tensile strength, cohesion and the frictional angle of rock masses in the Seyrantepe underground openings were also predicted from Mohr–Coulomb criterion. According to this criterion, the following relationships exist between cohesion, frictional angle, tensile strength and uniaxial compression strength.

$$\sigma_{cm} = \frac{2c_m\cos\phi_m}{1 - \sin\phi_m} \tag{1}$$

$$\sigma_{tm} = \frac{2c_m\cos\phi_m}{1 + \sin\phi_m} \tag{2}$$

Here, $\sigma_{cm}$, $\sigma_{tm}$, $c_m$ and $\phi_m$ are the uniaxial compression strength, tensile strength, cohesion and internal frictional angle of the rock mass, respectively. To estimate the uniaxial compression of the rock mass, the following empirical equations suggested by Aydan et al. (2012) were used.

$$\sigma_{\mathrm{cm}} = \frac{\mathrm{RMR}}{\mathrm{RMR} + 6(100 - \mathrm{RMR})}\sigma_{\mathrm{ci}} \tag{3}$$

In Eq. (3), $\sigma_{ci}$ is the average uniaxial compression strength of intact rock. After calculating the uniaxial compression strength of the rock mass, the cohesion was obtained from Eq. (1) by assigning an initial value to the frictional angle. The tensile strength was computed from Eq. (2) in terms of the obtained cohesion and frictional angle. Table 4 shows the geotechnical strength parameters calculated for RMR = 80 and the initial values of the frictional angle. As seen in Table 4, the Mohr–Coulomb criterion has greater tensile strength than that calculated from the Hoek–Brown criterion.

## Back analysis

To determine unknown geomechanical parameters, boundaries, or initial conditions, systems geometry, using observational methods such as measurement of field displacements, stresses or strains and back analysis techniques, is frequently used in geotechnical engineering projects (Sakurai et al. 2003; Ghorbani and Sharifzadeh 2009). Due to the rock masses being complicated and inhomogeneous material and containing discontinuities, it is difficult to obtain the mechanical parameters by considering only laboratory tests. Field tests are generally very expensive and are thus rarely conducted.

In terms of the required input data, the back analysis method can be classified into the stress back analysis method, deformation back analysis method and coupled back analysis method requiring both stress and deformation data. Although the methods present reasonable results by representing rock mass behaviour, installation of the test equipment to monitor the stress or deformation around the underground space can be troublesome.

**Table 4** Calculated rock mass geotechnical parameters with Mohr–Coulomb criterion

| Uniaxial compressive strength of the rock mass, $\sigma_{cm}$, (kPa) | Frictional angle of the rock mass, $\phi_m$, (°) | Cohesion of the rock mass, $c_m$, (kPa) | Tensile strength of the rock mass, $\sigma_{tm}$, (kPa) |
|---|---|---|---|
| 1632 | 35 | 424.8 | 442.3 |
| 1632 | 40 | 380.5 | 354.9 |
| 1632 | 45 | 338 | 280 |
| 1632 | 47.3 | 319 | 249 |

In this paper, an observational method to determine the shear and tensile strength parameters of rock masses was applied to section A-A' of the Seyrantepe underground openings. This method is performed by considering the failure zone of underground spaces. In this case, plastic zones in the numerical calculation output should give the failure zone shapes observed in the field. A direct approach employs the trial values of the unknown parameters as input data until the discrepancy between failure shapes observed in the field and corresponding failure shapes obtained from a numerical analysis is minimized. This failure-based back analysis procedure is continued until reasonable values of all variables are determined. Reasonable parameters are obtained by considering the failure shapes observed in the field. This approach is relatively simple and is suitable for determining the rock mass geotechnical parameters. Then, a stability analysis using these parameters can be performed.

Plaxis (2002) software was used to determine the shear strength parameters and tensile strength of the rock mass according to failure-based back analysis (Fig. 9). In the analysis, the unit weight and Poisson's ratio of the rock mass were considered the average values in Table 2 for dry core samples. A rock mass elastic modulus was calculated from the equation suggested by Hoek et al. (2002) and used as well. Afterwards, the cohesion, frictional angle and tensile strength of the rock mass were changed until the reasonable values were determined according to field observation. For averagely $c_m$ = 420 kPa, $\phi_m$ = 40° and $\sigma_{tm}$= 185 kPa, compatible results with the real failure shape along this section of the openings in the field were obtained. The values of unit weight, elastic modulus, Poisson's ratio, cohesion, internal frictional angle and tensile strength are presented in Table 5.

## Stability analysis of the Seyrantepe underground openings

To analyse and design underground spaces, there are a number of numerical, analytical and empirical techniques that can be used. Numerical approaches, such as the finite element, discrete element, or hybrid methods of analysis, are typically employed. Analytical solutions for the stability of near surface underground openings in rock masses are rarely used because of the inherently discontinuous nature of the problem. While empirical approaches are practical and easy to perform, they can be misleading in some cases. Therefore, each method has particular handicaps and advantages. The use of only one method is not reliable or economical enough to evaluate stability (Alejano et al. 2008). In this section, we present integrated numerical, analytical and empirical analyses to assess the stability of the Seyrantepe underground openings.

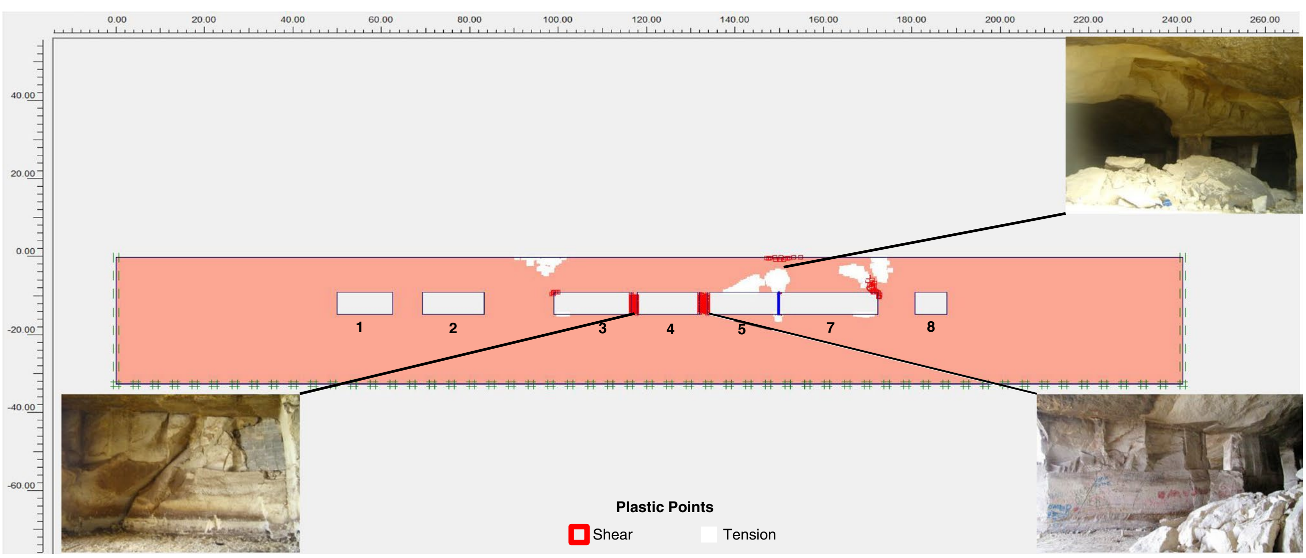


**Fig. 9** Failure-based back analysis for the prediction of unknown geotechnical parameters

**Table 5** Geotechnical properties of the rock mass based on back analysis

| Material | Unit weight, $\gamma$, (kN/m$^3$) | Elastic modulus, $E_m$, (GPa) | Poisson's ratio, $\nu$ | Cohesion, $c_m$, (kPa) | Frictional angle, $\phi_m$, (°) | Tensile strength, $\sigma_{tm}$, (kPa) |
|---|---|---|---|---|---|---|
| Limestone | 18.3 | 9.13 | 0.18 | 420 | 40 | 185 |

## FEM analysis

Plaxis (2002) software was used to model the underground openings. The sizes and material properties of the openings were considered input data for the software. Cross section A-A' was considered to evaluate stability. The geotechnical parameters given in Table 5 were used in a numerical analysis due to the results being compatible with the real failure shape observed in the field. Mohr–Coulomb failure criterion was governed to describe the failure behaviour of the rock. The in situ principal stresses ratio was considered to be 0.4 for this shallow soft rock mass. Because the ground water table is well below the base of the openings, the effect of pore water pressure was not included in the analysis. The vertical outer boundaries have horizontal fixity, while the horizontal base boundary has fixities in both the horizontal and vertical directions in the model. A 15-node triangular element and a very fine level of mesh were used to obtain higher quality stress distributions. Local refinements around the underground spaces were also made to improve the accuracy of the results. The wall located between openings 5 and 7 along section A-A', as seen in Fig. 6a, was included in the stability analysis. It was modelled as a plate element and represented by elastic behaviour in a numerical analysis. The modulus of elasticity and Poisson's ratio were assumed to be 2.5 GPa and 0.30, respectively, for the wall. The wall thickness was 0.2 m. The other mechanical properties of the wall required for numerical calculations are presented in Table 6.

**Table 6** Mechanical properties of the briquette wall

| Modulus of elasticity (GPa) | Wall thickness, d, (m) | EA (kN/m) | EI (kNm$^2$/m) | w (kN/m/m) | $\nu$ (Poisson's ratio) |
|---|---|---|---|---|---|
| 2.5 | 0.2 | $5\times10^5$ | $1.67\times10^3$ | 7 | 0.3 |

Figure 9 shows the plastic zones obtained from the analysis of section A-A'. Here, the elements that fail in shear are indicated in red, whereas yielded elements in tension are indicated in white with the Mohr–Coulomb failure criterion. As seen in Fig. 9, the roof between the pillars (between openings 4 and 5) and the briquette wall fails in tension. The rock pillars between openings 3 and 4 and between openings 4 and 5 fail in shear.

Maximum and minimum principal stress trajectories around the underground openings are presented in Fig. 10. The value of these principal stresses determines how the rock mass behaves to induced stresses. A comparative study of those principle stresses with different opening geometries may somehow help to predict the relative stability conditions. Figure 10 also illustrates a natural rock arch formation located at approximately ground level above the flat roof surface. A real loosened zone is formed below the natural rock arch, which cannot transmit any load to the supports.

This study also investigates the effects of the adjacent openings on failure and stability. For this purpose, the single isolated openings 5 and 7 are addressed. Figure 11 shows the failure zone around the opening without considering the adjacent openings. In this case, the tension failure zones are concentrated around the middle roof span of the opening and near the ground surface in the roof. The factor of safety

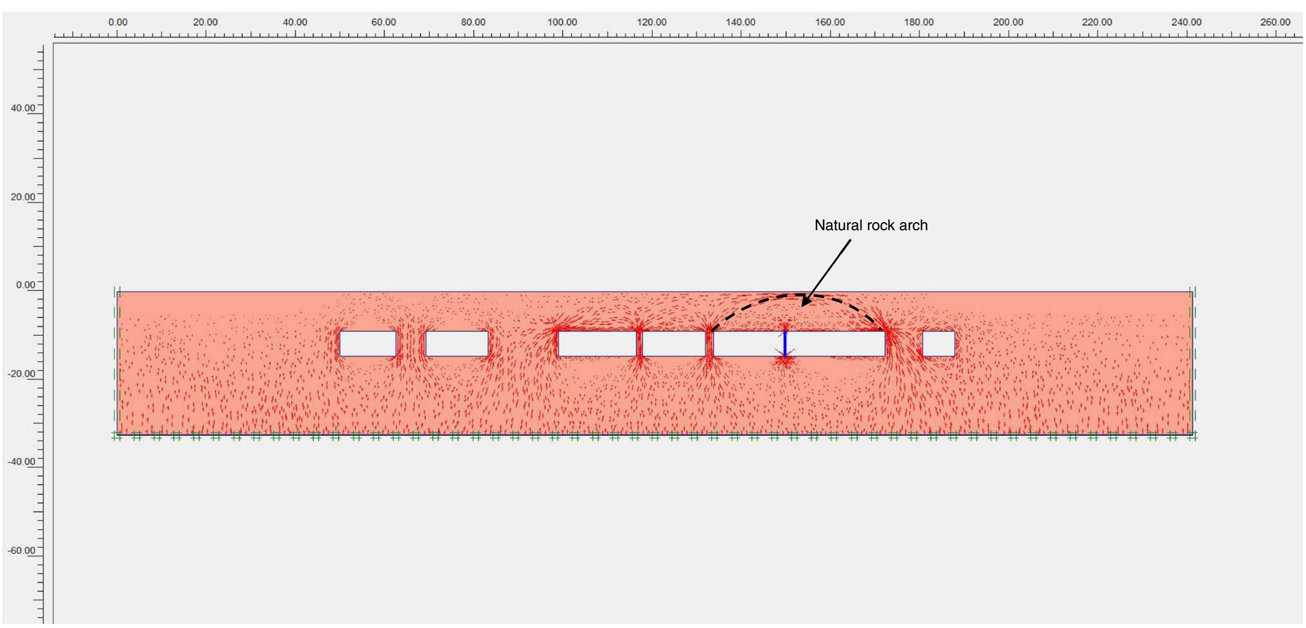


**Fig. 10** Principal stresses' trajectories

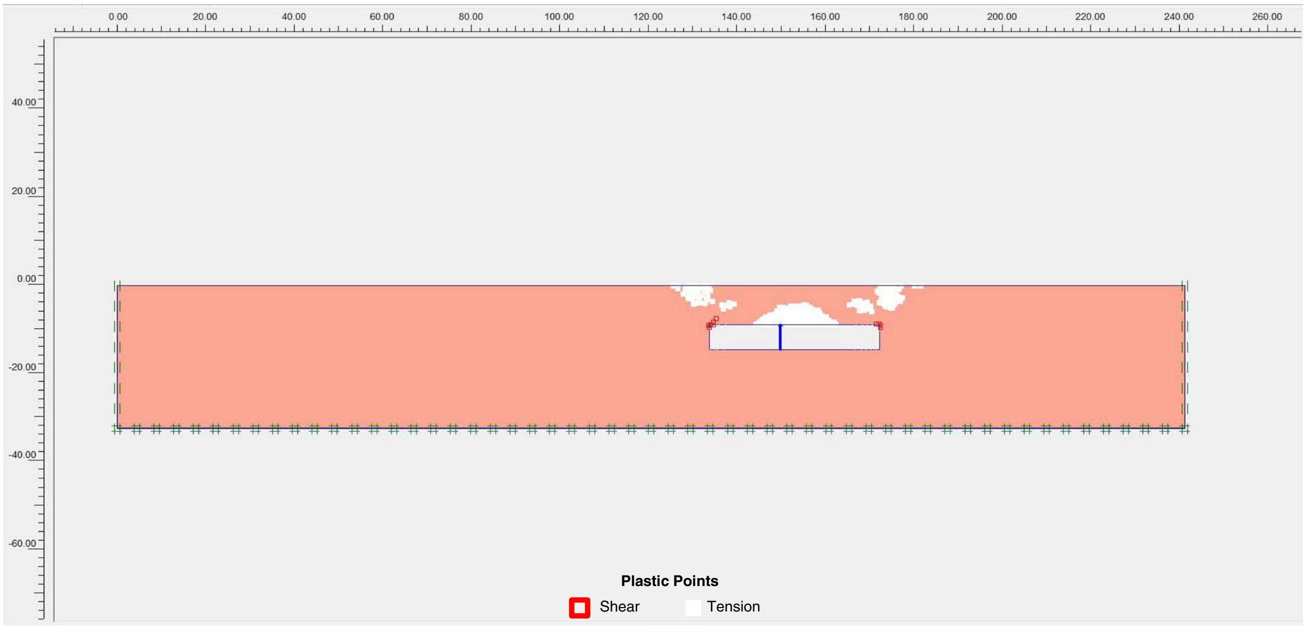


**Fig. 11** The failure zone around the openings 5 and 7 without considering the adjacent openings

against failure is calculated as 1.86. When considering the effects of the adjacent openings, plastic zones develop, as seen in Fig. 9. Tension failure zone develops towards the weaker pillars in the roof. Additionally, the weak pillars between openings 3 and 4 and between openings 4 and 5 fail in shear. The global factor of safety against failure of the openings is calculated to be 1.45 in this case.

## Analytical analysis

In this section, an analytical analysis method based on the beam bending theory was discussed to investigate the stability of the underground openings. Beam bending theories include fixed and simply supported beam analyses (Fig. 12a, b). When Euler Bernoulli's beam bending theory is applied to the roof of the openings, the limit of the roof span ($L$) under its dead weight ($q=\gamma\times h$) can be calculated by equating the maximum tension stress to tension strength. In this case, the limit of the roof span ($L$) is obtained from following equation.

$$\mathrm{L}=\sqrt{\frac{\beta\times h\times\sigma_{tm}}{\gamma}} \tag{4}$$

where $\sigma_{tm}$ is the tensile strength of the rock mass. $\beta$ takes the values of 2 and 4/3 for fixed and simply supported beams, respectively. The tensile strength of the rock mass can be calculated using the equation suggested by Aydan et al. (2012) as a function of the tensile strength of intact rock $\left(\sigma_{ti}\right)$ and the RMR value of the rock masses as follows:

$$\sigma_{tm}=\frac{\mathrm{RMR}}{\mathrm{RMR}+6(100-\mathrm{RMR})}\sigma_{ti} \tag{5}$$

Using the Eq. (4) and Eq. (5), the relationship between RMR and roof span was obtained for $\sigma_{ti}=462.5$ kPa (obtained from Eq. (5) for $\sigma_{tm}=185$ kPa and RMR = 80) and $\gamma=18.3$ kN/m$^3$, as seen in Fig. 13.

The average RMR value of the Seyrantepe underground openings is 80, as previously mention. As seen in Fig. 13, the limit of the roof span computed from a fixed beam approach is higher than that of a simply supported beam approach. For section A-A' of the Seyrantepe underground openings, which has a roof thickness of 9 m, the limit of the roof span is approximately 13.5 m for the fixed beam approach and 11 m for the simply supported beam approach. These analyses show that stability problems such as cracking and falling rock should be expected due to the larger roof spans measured along this section of the openings. This conclusion was in accordance with our observations.

A recently collapsed roof with a span of 38.5 m considered in FEM is also analysed using the bending theory with the fixed and simply supported beam approaches. The roof rock thickness is 9 m. Figure 14 shows the shear forces and bending moments along the beam. Figure 15 shows the normal stresses caused by bending moments. The compression strength of the rock mass is 1632 kPa for

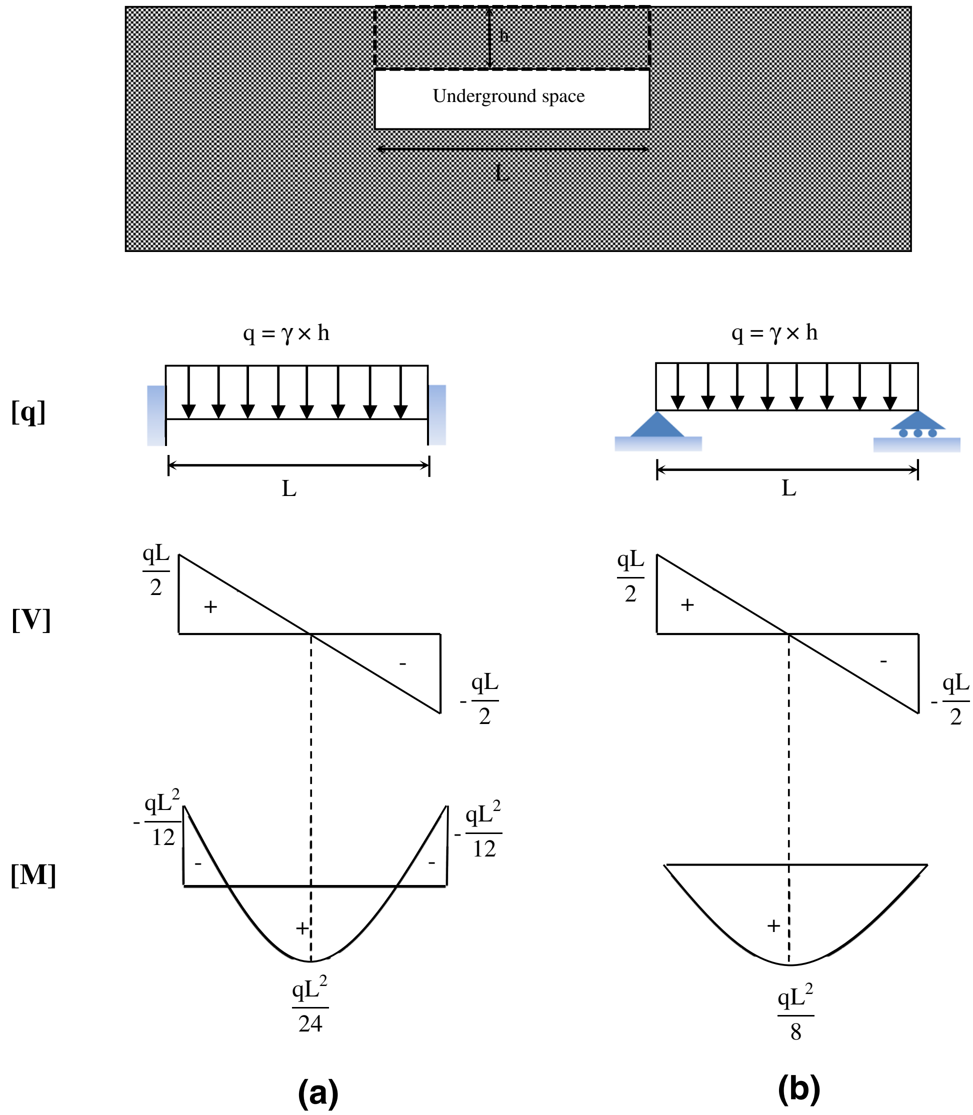


**Fig. 12** Illustrations of the mechanical models, distributed load [q], shear forces [V] and bending moments [M] for beam bending theory. **a** Fixed supported beam, **b** simply supported beam

an RMR of 80 according to Eq. (3). Due to the lack of tensile strength of the rock mass, back analysis results were considered in the bending theory to be 185 kPa. Normal stresses indicate that the compression stress ($\sigma_c$) exceeds the compression strength of the rock mass when the roof is considered to be only simply supported. In this case, crushing occurs at the upper surface of the roof around midspan. The tension stress ($\sigma_t$) of a simply supported beam exceeds the tension strength of the rock mass nearly all of the lower surface of the roof. As a result, tensile cracking should be expected on this surface. When considering the fixed beam approach, tensile stress exceeds tensile strength of the rock mass along the lower surface of the roof in a partially narrower area, and along the upper surface of the roof near the supports. In other words, stability problems caused by over-tension stresses should be expected at these locations.

## Empirical analysis

Empirical correlations based on rock mass quality can be used to determine the limit span or diameter of underground excavations. Barton et al. (1974) evaluated more than 200 case records and suggested an equation between unsupported span and the Tunneling Quality Index (Q) by considering the degree of safety, type of excavation and stand-up time. These requirements to determine the unsupported design span are represented as excavation support ratio (ESR) value in the equation. The ranges of the ESR values for the type of excavation can be seen in Barton et al. (1974). Then, a similar equation was proposed by Kaiser et al. (1986) for the RMR classification system. Recent studies were performed by Aydan and Tokashiki (2011). Based on their observation of natural limestone

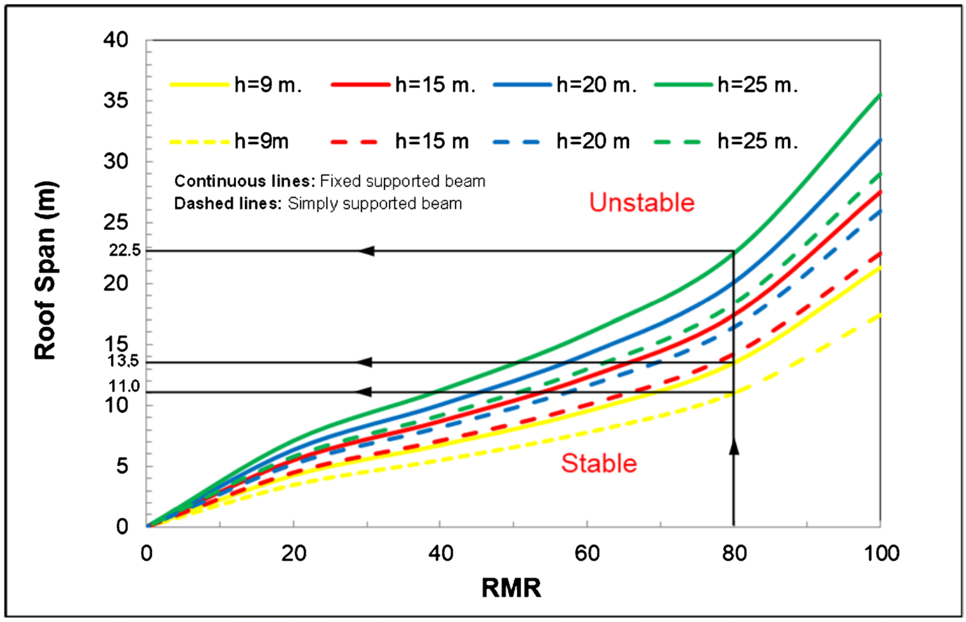


**Fig. 13** Stability assessment chart of the Seyrantepe underground openings with Euler Bernoulli bending theory

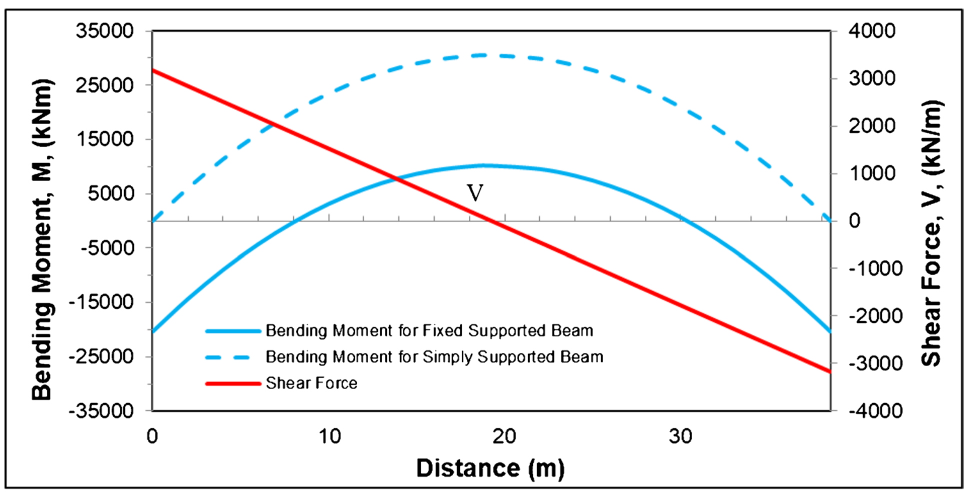


**Fig. 14** Shear forces and bending moments for the recently collapsed roof span

caves on Ryukyu Island, the authors determined four stability classes, namely stable, local unstable, considerably local unstable and unstable. The boundaries of each class are drawn by the following two equations to determine the limit of the roof span as a function of RMR with linear and power functions.

$$L = a.RMR + b \text{ (as linear function)} \quad (6)$$

$$L = a.RMR^{b} \text{ (as power function)} \quad (7)$$

where $a$ and $b$ are the empirical coefficients that can be obtained from Aydan and Tokashiki (2011) for each boundary of the stability classes.

The equations suggested by these studies are given in Table 7. Barton et al. (1974) suggested using the value of ESR as 1.3 for excavation categories such as storage rooms, surge chambers and access tunnels. The analysis was executed by taking the value of ESR as 1.3. The average RMR and Q values were used in the equations. The data obtained for RMR and the spans of the Seyrantepe underground quarry were plotted on the Aydan and Tokashiki (2011) stability graph (Fig. 16). The position of the quarry is indicated by a straight line. As seen here, the Seyrantepe underground openings are located in stable (I) and local unstable (II) zones. Recently, roof collapse observed in opening 5 is in a local unstable zone, and

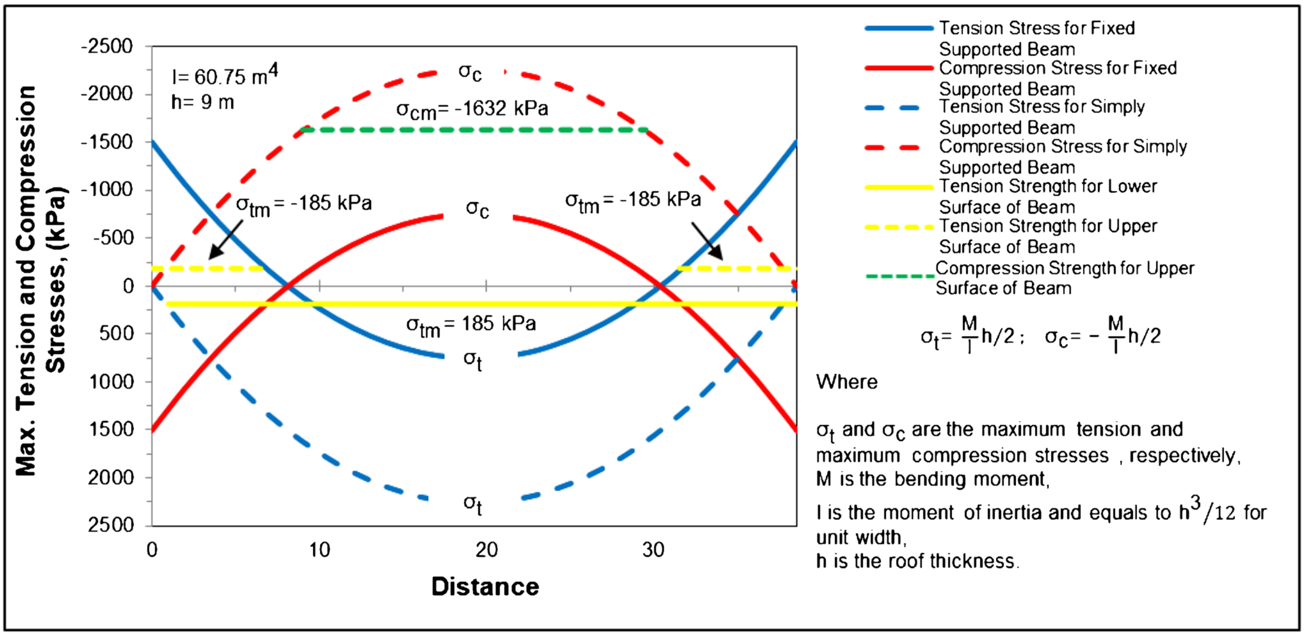


**Fig. 15** Normal stresses caused by bending theory along the recently collapsed roof span

**Table 7** The equations for the limit of the roof span using in empirical analysis

| References | Equations | Notes | Limit span, L (m) |
|---|---|---|---|
| Barton et al. (1974) | $L = 2 \times ESR \times Q^{0,4}$ | ESR = 1.3<br>Q = 57.6 | 13.2 |
| Kaiser et al. (1986) | $L = ESR \times \exp(\frac{RMR-25}{22})$ | ESR = 1.3<br>RMR = 80 | 15.8 |
| Aydan and Tokashiki (2011) | L = a.RMR + b<br>$L = a.RMR^{b}$ | I–II: a = 1.2; b = -60<br>II–III: a = 3.0; b = -120<br>III–IV: a = 4.3; b = -130<br>I–II: a = 0.001; b = 2.4<br>II–III: a = 0.003; b = 2.4<br>III–IV: a = 0.005; b = 2.4 | 36<br>120<br>214<br>36.9<br>110.8<br>184.7 |

the Seyrantepe underground openings are mostly stable, depending on the span and RMR value. Figure 17 compares the limit of the roof spans based on the equations given in Table 7. The spans of the Seyrantepe underground quarry range between 5 and 55 m. According to Barton et al. (1974), the limit of the roof span is calculated as 13.2 m. According to Kaiser et al. (1986), it is 15.8 m. The observations show that there are many spans greater than those calculated by Barton et al. (1974) and Kaiser et al. (1986), and they are still stable or local unstable. Figure 17 implies that the equations of Barton et al. (1974) and Kaiser et al. (1986) give conservative results for the Seyrantepe underground openings.

## Conclusions

This paper presents a stability assessment of the Seyrantepe underground openings and discusses its implications in geotechnical engineering. To determine the geotechnical parameters of the rock mass, experimental numerical and theoretical studies suggested by various researchers were carried out. Integrated numerical, empirical and analytical methods were undertaken to investigate the stability.

The experimental results and visual site characterization study showed that although the limestone surrounding

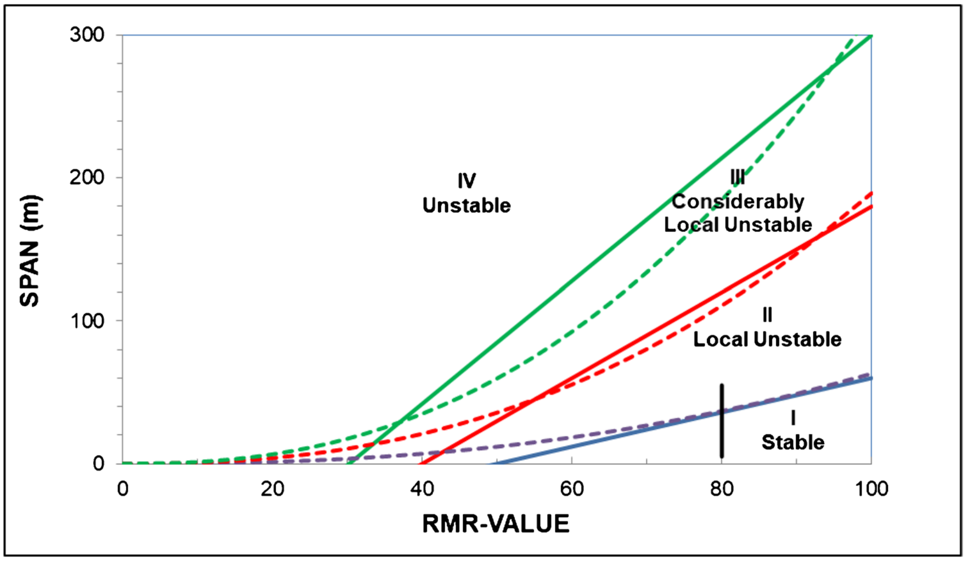


**Fig. 16** Stability graph based on the equations of Aydan and Tokashiki (2011)

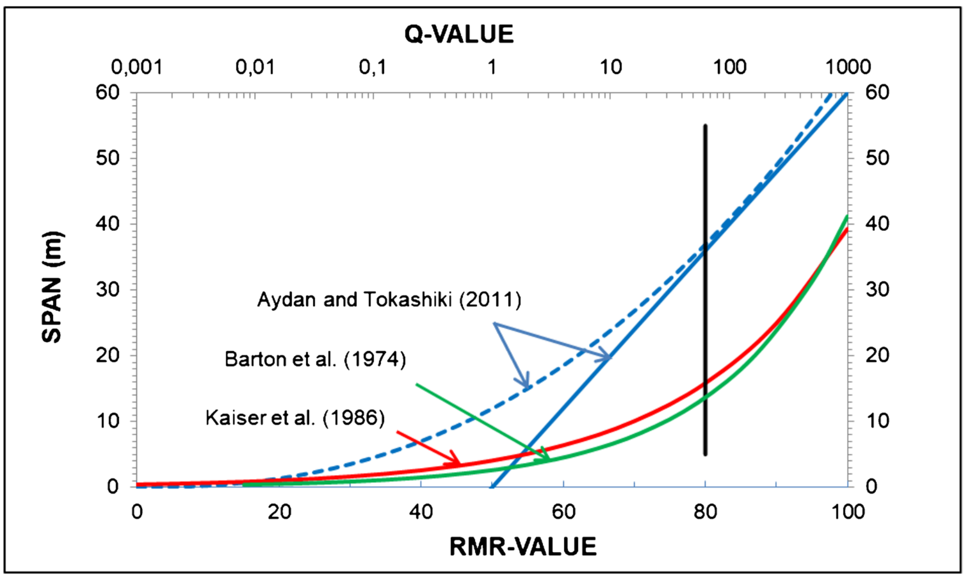


**Fig. 17** Comparison of the limit of the roof spans based on the equations given in Table 7

the openings is a good-quality rock mass, it is a weak rock in terms of intact rock strength. The strength of the rock is drastically reduced under saturated conditions. It is expected that the alteration and process of freezing–thawing accelerates further degradation of the rock and affects the openings' stability. Furthermore, more detailed studies are recommended for long-term stability in view of the effects of degradation due to wetting–drying and freezing–thawing processes and the time-dependent characteristics of the surrounding rock mass.

The results of the combined analysis showed that Mohr–Coulomb criterion gives the highest tensile strength and that the lowest tensile strength is obtained from Hoek–Brown criterion. Cohesion is similar for both failure criteria. Failure-based back analysis seems quite promising to determine the cohesion, frictional angle and tensile strength of the rock mass.

The numerical analyses showed that adjacent spans affect the stability, failure mechanism (shear or tension) and failure places. When considering a single isolated opening, the factor of safety against failure is calculated to be greater than that considered for adjacent openings. Tension failures occur around the midspan and at the places near the ground surface of the roof for a single isolated opening. When considering the adjacent openings, tension failure zones in the roof develop towards the weaker pillars. In other word, weaker pillars determine the failure mechanism of the roof.

According to the bending theory, the limit of the roof span ranges between 11 and 22.5 m depending on a roof thickness of 9 and 25 m, respectively, for the RMR of rock masses. Rock masses behave elastically up to these values. When the span is greater, the rock mass will yield, and plastic zones will occur. The fixed supported beam bending theory indicates that the tensile stress exceeds tensile strength of the rock mass both along the lower surface of the roof in a partially narrower area than simply supported beam bending theory and along the upper surface of the roof near the supports. According to both bending theory, plastic tensile zones are expected around midspan, and this conclusion is in accordance with finite element method analysis.

The empirical functions proposed by Barton et al. (1974) and Kaiser et al. (1986) gave more conservative results compared with Aydan and Tokashiki (2011). A recently collapsed roof observed in opening 5 is in a local unstable zone, and the Seyrantepe underground openings are mostly stable, according to Aydan and Tokashiki (2011). This situation corresponds to the stability categories observed in the underground openings. Therefore, it can be said that the empirical functions proposed by Aydan and Tokashiki (2011) performed much better than others when evaluating the stability categories of the Seyrantepe underground openings.

**Acknowledgements** The authors thank to the Gaziantep Metropolitan Municipality for the kind help and support provided.

## Declarations

**Conflict of interest** The authors declare no competing interests.

## References

Alejano LR, Taboada J, García-Bastante F, Rodriguez P (2008) Multi-approach back-analysis of a roof bed collapse in a mining room excavated in stratified rock. Int J Rock Mech Min Sci 45:899–913. https://doi.org/10.1016/j.ijrmms.2007.10.001

Aydan Ö, Tokashiki N (2011) A comparative study on the applicability of analytical stability assessment methods with numerical methods for shallow natural underground openings. In: The 13th International Conference of the International Association for Computer Methods and Advances in Geomechanics, Melbourne, Australia, pp. 964–969

Aydan Ö, Geniş M, Tokashiki N (2012) Some consideration on yield (failure) criteria in rock mechanics. In: The 46th US Rock Mechanics/Geomechanics Symposium, American Rock Mechanics Association, 24–27 June 2012, Chicago, IL

Aydan Ö, Ulusay R, Tokashiki N (2014) A new rock mass quality rating system: RockMass Quality Rating (RMQR) and its application to the estimation of geomechanical characteristics of rock masses. Rock Mech Rock Eng 47(4):1255–1276. https://doi.org/10.1007/s00603-013-0462-z

Barton NR, Lien R, Lunde J (1974) Engineering classification of rock masses for the design of tunnel support. Rock Mech 6:189–239. https://doi.org/10.1007/BF01239496

Bieniawski ZT (1989) Engineering rock mass classifications. Wiley, New York

Canakci H (2007) Collapse of caves at shallow depth in Gaziantep city center, Turkey: a case study. Environ Geol 53:915–922. https://doi.org/10.1007/s00254-007-0802-y

Coskun B, Coskun B (2000) The Dead Sea Fault and related subsurface structures, Gaziantep Basin, southeast Turkey. Geol Mag 137:175–192. https://doi.org/10.1017/S0016756800003770

Deere DU, Miller DW (1967) The rock quality designation (RQD) index in practice, classification systems for engineering purposes. American Society for Testing and Materials, Philadelphia, ASTM STP, pp 91–101

Ghorbani M, Sharifzadeh M (2009) Long term stability assessment of Siah Bisheh Powerhouse cavern based on displacement back analysis method. Tunn Undergr Sp Technol 24:574–583. https://doi.org/10.1016/j.tust.2009.02.007

Grimstad E, Barton N (1993) Updating of the Q-system for NMT. In: Proceedings on International Symposium on Sprayed Concrete, Fagernes, Norway. Norwegian Concrete Association, Oslo, 22–26 October 1993, pp 46–66

Hatzor YH, Wainshtein I, Mazor DB (2010) Stability of shallow karstic caverns in block rock masses. Int J Rock Mech Min Sci 47:1289–1303. https://doi.org/10.1016/j.ijrmms.2010.09.014

Hoek E (1994) Strength of rock and rock masses. ISRM News Journal 2(2):4–16

Hoek E (2007) Practical Rock Engineering. https://www.rocscience.com/assets/resources/learning/hoek/Practical-Rock-Engineering-Full-Text.pdf. Accessed 5 Aug 2021

Hoek E, Brown ET (2019) The Hoek–Brown failure criterion and GSI – 2018 edition. J Rock Mech Geotech Eng 11:445–463. https://doi.org/10.1016/j.jrmge.2018.08.001

Hoek E, Kaiser PK, Bawden WF (1995) Support of underground excavations in hard rock. Balkema, Rotterdam

Hoek E, Marinos PG (2000) Predicting tunnel squeezing problems in weak heterogeneous rock masses. Tunnels and Tunnelling International 132(11):45–51

Hoek E, Carranza-Torres CT, Corkum B (2002) Hoek-Brown failure criterion-2002 edition. International Proceedings of the 5th North American Rock Mechanics Symposium, Toronto, pp 267–273

ISRM (2007) The complete ISRM suggested methods for rock characterization, testing and monitoring: 1974–2006. In: Ulusay R, Hudson JA (eds), suggested methods prepared by the ISRM commission on testing methods. Compilation arranged by the ISRM Turkish National Group. Kozan Ofset, Ankara, p 628

Kaiser PK, Mackay C, Gale AD (1986) Evaluation of rock classification at B.C. Rail Tumbler Ridge Tunnels. Int J Rock Mech Rock Eng 19:205–234

Lauffer H (1958) Gebirgsklassifizierung Für Den Stollenbau Geol Bauwesen 24:46–51

MTA (1997) Geological map of the Gaziantep-K24 quadrangle. General Directorate of Mineral Research And Exploration, Ankara

PLAXIS 2D v8.2, (2002) Finite element program, developed for the analysis of deformation, stability and groundwater flow in geotechnical engineering. Delft, Netherlands

Rocscience (2002) RocLab (v.1.0) Rock mass strength analysis using the generalized Hoek-Brown failure criterion

Sakurai S, Akutagawa S, Takeuchi K, Shinji M, Shimizu N (2003) Back analysis for tunnel engineering as a modern observational method. Tunn Undergr Sp Technol 18:185–196. https://doi.org/10.1016/S0886-7798(03)00026-9

Sonmez H, Ulusay R (2007) Engineering properties of rock masses, 2nd edn. vol 60. TMMOB Chamber of Geological Engineers of Turkey, Ankara, p. 292 (in Turkish)

Suchowerska AM, Merifield RS, Carter JP, Clausen J (2012) Prediction of underground cavity roof collapse using the Hoek-Brown failure criterion. Comput Geotech 44:93–103. https://doi.org/10.1016/j.compgeo.2012.03.014

Terlemez I, Şentürk K, Ateş Ş, Sümengen M, Oral A (1992) Geology of between Gaziantep region and Pazarcık-Sakçagöz-Kilis Elbeyli-Oğuzeli. MTA, Report: 9526, Ankara

Terlemez I, Şentürk K, Sümengen M, Oral A (1997) Turkey geological maps No: 45. Geological Studies Department, MTA, Ankara (in Turkish)

Tolun N, Pamir HN (1975) Explanatory text of the geological map of Turkey-Hatay. MTA, Ankara

Ulusay R, Aydan Ö, Geniş M, Tano H (2013) Stability assessment of Avanos Underground Congress Centre (Cappadocia, Turkey) in soft tuffs through an integrated scheme of rock engineering methods. Int J Rock Mech Rock Eng 46:1303–1321. https://doi.org/10.1007/s00603-012-0363-6

Waltam AC, Park HD (2002) Roads over lava tubes in Cheju Island, South Korea. Eng Geol 66:53–64. https://doi.org/10.1016/S0013-7952(02)00030-3

Wickham GE, Tiedemann HR, Skinner EH (1972) Support determination based on geologic predictions. In: North American rapid excavation tunneling conference, Chicago, pp 43–64